Elastic moduli of body-centered cubic lattice near rigidity percolation threshold: Finite-size effects and evidence for first-order phase transition

Sepehr Arbabi[1,*] and Muhammad Sahimi[2,†]

[1]*Department of Chemical Engineering, The University of Texas Permian Basin, Odessa, Texas 79762, USA*

[2]*Mork Family Department of Chemical Engineering and Materials Science, University of Southern California, Los Angeles, California 90089-1211, USA*

(Received 10 November 2020; revised 22 March 2021; accepted 2 April 2021; published 19 April 2021)

Extensive numerical simulations of rigidity percolation with only central forces in large three-dimensional lattices have indicated that many of their topological properties undergo a first-order phase transition at the rigidity percolation threshold p_{ce}. In contrast with such properties, past numerical calculations of the elastic moduli of the same lattices had provided evidence for a second-order phase transition. In this paper we present the results of extensive simulation of rigidity percolation in large body-centered cubic (bcc) lattices, and show that as the linear size L of the lattice increases, the elastic moduli close to p_{ce} decrease in a stepwise, discontinuous manner, a feature that is absent in lattices with $L < 30$. The number and size of such steps increase with L. As p_{ce} is approached, long-range, nondecaying orientational correlations are built up, giving rise to compact, nonfractal clusters. As a result, we find that the backbone of the lattice at p_{ce} is compact with a fractal dimension $D_{bb} \approx 3$. The absence of fractal, scale-invariant clusters, the hallmark of second-order phase transitions, together with the stairwise behavior of the elastic moduli, provide strong evidence that, at least in bcc lattices, many of the topological properties of rigidity percolation as well as its elastic moduli may undergo a first-order phase transition at p_{ce}. In relatively small lattices, however, the boundary effects interfere with the nonlocal nature of the rigidity percolation. As a result, only when such effects diminish in large lattices does the true nature of the phase transition emerge.

DOI: 10.1103/PhysRevE.103.042314

I. INTRODUCTION

Rigidity percolation (RP) was introduced by Thorpe [1] and Feng and Sen [2]. In its simplest version the RP represents percolation on elastic networks with central (stretching) forces (CFs), which is described by the following Hamiltonian:

$$\mathcal{H} = \frac{1}{2}\sum_{j\in\{i\}} e_{ij}[(\mathbf{u}_i - \mathbf{u}_j)\cdot\mathbf{R}_{ij}]^2 , \tag{1}$$

where $\mathbf{u}_i$ is the displacement of site i, e_{ij} is the force constant of bond ij, $\mathbf{R}_{ij}$ is a unit vector from i to j, and the sum is over all sites j that are nearest neighbors of site i. Thorpe [1] and Feng and Sen [2] showed that the rigidity percolation threshold p_{ce}^B for bond disorder is much larger than p_c^B, the connectivity threshold of scalar percolation. For example, for a d-dimensional cubic network one has $p_{ce}^B = 1$. Thus, study of the RP in lattices with only nearest-neighbor connections has been restricted mostly to those for which $p_{ce}^B < 1$, e.g., the triangular and body-centered cubic (bcc) networks. For brevity, we delete the superscript B and refer to the bond-percolation threshold in the RP as p_{ce}. Rigidity percolation may also include bond-bending forces [3–6], but the focus of the present paper is on lattices with only CFs.

An effective-medium approximation (EMA) for the elastic moduli of a network in the RP model predicted [7–13] that $p_{ce} = 2d/Z$, where d and Z are, respectively, the dimensionality and coordination number of the lattice. The same result is obtained when one uses the constraint-counting method [1]. Note that $p_{ce}Z$ is the average coordination number of a d-dimensional lattice at p_{ce}. Thus, the EMA indicates that the coordination number of such a lattice must be greater than $2d$ in order for it to have nonzero elastic moduli.

Rigidity percolation in two-dimensional (2D) lattices has been studied [14–20] extensively, although the nature of the phase transition in 2D RP is still to some extent controversial. In a d-dimensional CF lattice, no element of the structure can be moved in any direction with respect to the rest of the lattice, nor can it be rotated along $\frac{1}{2}d(d-1)$ independent axes [21], implying that there are $\frac{1}{2}d(d+1)$ constraints on the possible motion of each element of the rigid lattice. Therefore, there are long-range, nondecaying orientational correlations in rigidity percolation.

The existence of such long-range correlations provides an important hint about the nature of phase transition in the sample-spanning rigid cluster at p_{ce}, because such correlations give rise, in the thermodynamic limit, to clusters that, after averaging, are translationally, but not scale, invariant [22,23]. Since scale-invariant structures at a transition point represent the signature of second-order phase transitions, the conclusion is that the RP transition may be first order.

Using large-scale simulations, Moukarzel *et al.* [24] provided further numerical evidence in support of the conclusion. Moreover, by solving the problem on the Bethe lattices, which

*sepehr.arbabi@utpb.edu

†moe@usc.edu

corresponds to the mean-field limit of percolation at its upper critical dimension, they found [25] that, at least in some cases, the percolation transition in the sample-spanning rigid cluster at p_{ce} is first order, and that some variations of the problem are similar to bootstrap percolation [26,27] that, in certain limits, also gives rise to a first-order phase transition. Earlier, Sahimi and Ray [28] had suggested that bootstrap percolation may be relevant to describing mechanical properties of disordered lattices.

But if the topological properties of a sample-spanning rigid cluster with CFs undergo a first-order phase transition at p_{ce}, then interpretation of the power laws that govern the elastic moduli of the CF percolation networks that are characteristic of second-order phase transitions becomes problematic. A possible resolution of the contradiction may be as follows: Although the sample-spanning CF cluster may be compact (and, hence, the phase in transition in its properties may be first order), its *backbone* is not [24], and may in fact be a fractal object with a well-defined fractal dimension [24], $D_{bb} \approx 1.78$, for 2D CF clusters. Due to the fractality of the rigid backbone, the RP transition, defined as the point at which the elastic moduli vanish, is also second order.

Jacobs and Thorpe [14,29] computed the critical exponents ν_e and β_e that characterize, respectively, the divergence of the RP correlation length ξ_p near p_{ce}, $\xi_p \sim (p - p_{ce})^{-\nu_e}$, and vanishing of the percolation fraction $P(p)$ (the fraction of bonds in the sample-spanning cluster) near p_{ce}, $P(p) \sim (p - p_{ce})^{\beta_e}$, as well as the fractal dimensions D_f and D_{bb}, with D_f being the fractal dimension of the rigid sample-spanning cluster at p_{ce}. Their estimates for 2D networks were $\nu_e \simeq 1.21$, $\beta_e \simeq 0.175$, and $D_f \simeq 1.86$, consistent with a geometrical second-order phase transition at p_{ce}. Their estimate, $D_{bb} \simeq 1.8$, was consistent with that of Moukarzel *et al.* [24]. However, there are still 2D cases for which the RP transition at p_{ce} is believed to be first order, such as the random-bond model [30] and networks with chemical order [31], but Chubynsky and Thorpe [32] still contended that, "up to now, there have been no cases where it [first-order transition] would be observed for a regular randomly diluted network."

In contrast to the RP with CFs in 2D lattices, as well as those with the CF and bond-bending forces in both two and three dimensions that have been studied extensively [3–6,33–35], RP with the CFs alone has not been extensively studied in three-dimensional (3D) lattices. In fact, the only studies that the authors are aware of are their own [17] and that of Chubynsky and Thorpe [32]. The latter stated that "the rigidity percolation transition on such networks [BCC lattices] is first order, in contrast to bond-bending networks in 3D and central-force networks in 2D. In fact, the transition is actually first order geometrically, but second order physically, as it is known from previous work that the elastic constants change continuously at the transition [point]."

Chubynsky and Thorpe [32] studied only the connectivity of the bcc lattice, and did not compute its elastic moduli. On the other hand, the present authors' results for the elastic moduli of the bcc lattice [17], which had been obtained with relatively small lattices, had indicated that the elastic moduli undergo a second-order phase transition. Therefore, given the results and contention of Chubynsky and Thorpe, it is still an open question whether the elastic moduli of bcc lattices in the RP with only the CFs undergo a first- or second-order phase transition at p_{ce}.

The purpose of the present paper is, therefore, to study the RP with the CFs in a bcc lattice by simulating systems much larger than what had been done in the past, and to examine whether the elastic moduli of the lattice undergo a second- or first-order transition at p_{ce}. In particular, we study finite-size effects as the size of the lattice increases, and how they affect the elastic moduli.

The rest of this paper is organized as follows. In Sec. II we describe how the force distribution is used to compute various quantities of interest, followed in Sec. III by the details of the numerical simulations. The results are presented and discussed extensively in Sec. IV, while the paper and its results are summarized in Sec. V.

II. FORCE DISTRIBUTION

As first pointed out by Sahimi and Arbabi [33], a fruitful approach to investigating the RP is by studying the force distribution (FD), the distribution of the forces that the intact (uncut) bonds of a network withstand. To determine the FD, one imposes a given boundary condition on the network and determines the nodal displacements $\mathbf{u}_i$ by minimizing the elastic energy given by Eq. (1), from which the total force F_i exerted on a bond i and, thus, its distribution, are calculated. Of particular interest are the moments of the FD defined by

$$M_q = \sum_i n_{F_i} F_i^q, \tag{2}$$

where n_{F_i} is the number of bonds that suffer a force with magnitude F_i. If the rigidity transition with the CFs is second order, then, near p_{ce}, the moments M_q should follow the power law,

$$M_q \sim (p - p_{ce})^{\tau_q} \sim \xi_p^{-\tau_q/\nu_e}, \tag{3}$$

where all the τ_q are distinct [33]. For length scales $L \ll \xi_p$ one should replace ξ_p by L and, therefore,

$$M_q \sim \text{Ł}^{-\tilde{\tau}_q}, \tag{4}$$

where $\tilde{\tau}_q = \tau_q/\nu_e$. Only nonzero values of F_i contribute to M_q and, therefore, M_0 is simply the total number of bonds in the backbone of the lattice. As a result, $-\tilde{\tau}_0$ is simply the fractal dimension D_{bb} of the backbone of the sample-spanning rigid cluster. On the other hand, M_1 is the average force that a bond withstands, and M_2 is proportional (and, depending on the type of the lattice, is exactly equal) to the elastic moduli of the network. Thus, if the rigidity transition for the elastic moduli G of the lattice is second order, so that we can write

$$G \sim (p - p_{ce})^f, \tag{5}$$

then $f = \tau_2$. One main goal of this paper is to check whether power law (5) holds for bcc lattices, and whether it is unambiguously valid as the size of the lattice increases.

III. DETAILS OF NUMERICAL SIMULATIONS

To compute the FD we minimized the elastic energy $\mathcal{H}$ with respect to the displacement $\mathbf{u}_i$; i.e., we set $\partial\mathcal{H}/\partial\mathbf{u}_i = 0$. Writing down this equation for every interior node of the

network results in $3N$ simultaneous linear equations for the nodal displacements $\mathbf{u}_i$ of the network of N internal nodes. We computed the shear modulus $\mu = C_{44}$ of the lattice, where C_{44} refers to the entry of the stiffness tensor $\mathbf{C}$ and, therefore, imposed shearing boundary condition in one direction and periodic boundary conditions in the other directions. The resulting set of linear equations was solved by the adaptive accelerated Jacobi-conjugate gradient method that uses an acceleration parameter optimized for each iteration. The convergence criterion was that for all the sites i, $|[\mathbf{u}_i^{(k)} - \mathbf{u}_i^{(k-1)}]/\mathbf{u}_i^{(k-1)}| < \epsilon$, where $\mathbf{u}_i^{(k)}$ is the displacement of site i after the kth iteration; we set $\epsilon = 10^{-5}$.

Since a main goal of the study is to understand finite-size effects, we simulated $L \times L \times L$ lattices with $L = 10$, 12, 14, 16, 18, 20, 30, 40, 50, 56, 60, 62, 64, 66, 68, and 70, where L is the number of nodes in a direction at the corner of the elementary cubes in the lattice. In our previous study [17] we had simulated bcc lattices with up to $L = 16$. For each L a large number of realizations were generated and simulated, ranging from 10^3 for $L = 10$ to 50 for $L = 70$. The lattice with $L = 70$ has 328 509 nodes, almost three times larger than the largest lattice simulated by Chubynsky and Thorpe [32] and the largest 3D lattice that we are aware of simulated in such studies.

IV. RESULTS AND DISCUSSION

We carried out extensive numerical simulation of RP with CFs on a bcc lattice. In what follows we present the results and discuss their implications.

A. The percolation threshold

As is well known [15,17], if the transition of the elastic moduli of rigid lattices with CFs at p_{ce} is second order, then accurate estimates of the scaling exponents that characterize the power-law behavior of the elastic near p_{ce}, Eq. (3), depend sensitively on precise estimates of p_{ce}. Although constraint counting and the EMA do provide estimates of p_{ce}, they are not accurate enough for use in the present analysis. We had previously proposed [17] a method for obtaining precise estimates of p_{ce}, which was based on the moments of the FD and is as follows. If, in a network of linear size L with a fraction p of intact springs, one calculates the ratio $r_{2,1} = M_2/M_1$ for various values of L and p, with M_1 and M_2 being the first two moments of the FD distribution, then at the true value of p_{ce} a plot of $\ln r_{2,1}$ versus $\ln L$ should be a straight line. In principle, this should be true for any ratio, $r_{q,q-1} = M_q/M_{q-1}$, but for $q > 2$, the moments of the FD are subject to large fluctuations. This method was tested [17] for the triangular network with network sizes $L = 25$, 35, 45, and 55 and a few values of p, $0.636 \leqslant p \leqslant 0.65$. The plot of $\ln r_{2,1}$ versus $\ln L$ turned out to be a straight line only if $0.640 < p < 0.642$. Thus, the estimate, $p_{ce} \simeq 0.641 \pm 0.001$, was obtained, in complete agreement with the most accurate estimate of p_{ce}.

A bcc lattice of CF springs is also rigid with respect to a transverse shear, as well as a volume change and, therefore, it should possess a well-defined $p_{ce} < 1$. Note, however, that with pure elongational shear along the cubic axis, the bcc lattice would have no restoring elastic constant. Thus, the moment method was also used [17] to study bond percolation on the bcc lattice with CFs. It turned out that the plot of $\ln r_{2,1}$ versus $\ln L$ would be linear only if $p_{ce} \simeq 0.737$, but not for $p < 0.735$ or $p > 0.739$. To check our old results, we carried out new computations with $L = 10$, 20, 30, and 40. The number of realizations varied from 2000 for $L = 10$ to 40 for $L = 40$. Figure 1 presents the results. The three plots indicate that the data for $\ln(M_2/M_1)$ versus p are most accurately on a straight line for $p \simeq 0.737$. Linearity of the plot for $p \simeq 0.741$ is also very close to $p \simeq 0.737$, whereas the data do not form a straight line for $p \simeq 0.733$. Thus, this confirms our earlier result: for bond percolation on a bcc lattice with CFs, $p_{ce} \simeq 0.737 \pm 0.004$, much larger than $p_c \simeq 0.1795$ for scalar bond percolation on the same network.

Chubynsky and Thorpe [32] estimated that $p_{ce} \simeq 0.7485$. They acknowledged, however, that their lattice is different from a bcc lattice, stating that the difference "is probably due to the fact that their [our] simulations were on undistorted nongeneric lattices." Since their estimate of p_{ce} is larger than our estimates, the results that are described and discussed below also include lattices at their particular value of p_{ce}. Despite this, we also carried out some computations with the estimate of p_{ce} that Chubynsky and Thorpe [32] reported. But, aside from the decrease of the shear modulus μ with the size L at their p_{ce}, we found no particular feature in the behavior of $\mu(L)$ at that point.

B. Finite-size effects: Stairwise variation of the elastic modulus

Let us point out that the EMA and our earlier numerical simulations with $L = 16$ had provided no hint about the possibility of a first-order phase transition for the elastic modulus μ at p_{ce}. Figure 2 compares the numerical results (for $L = 16$) with the predictions of the EMA, both of which indicate a continuous phase transition at p_{ce}.

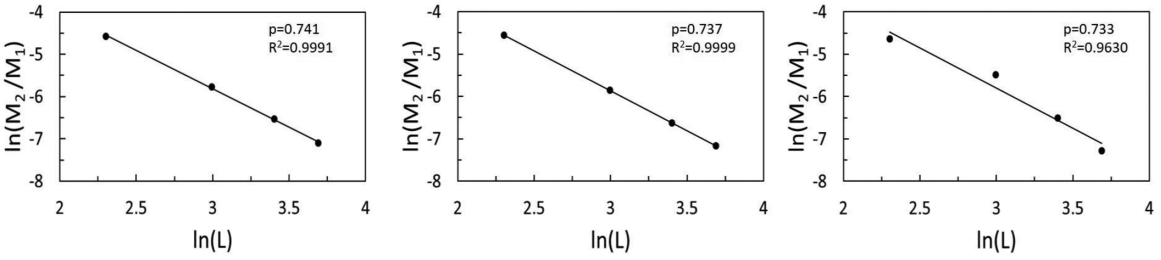

FIG. 1. Logarithmic plot of M_2/M_1, the ratio of the first two moments of the force distribution, versus the linear size L of the bcc lattice, for three values of p, together with the associated values of the goodness of the fit R^2. Note the deviation from linearity for $p = 0.733$.

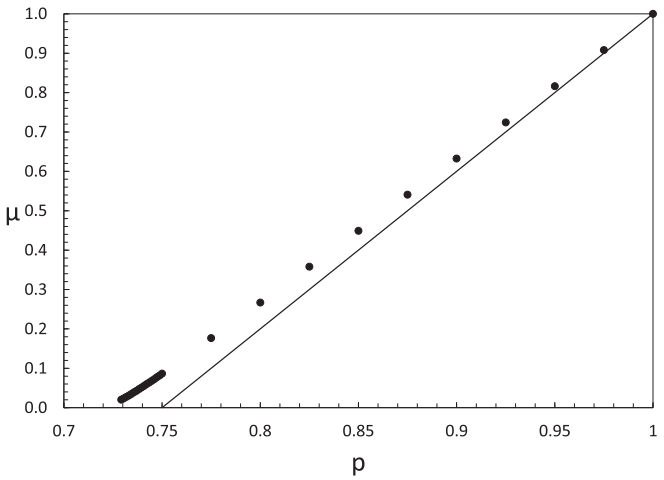

FIG. 2. Comparison of the calculated shear modulus of the bcc lattice (circles) with a linear size of $L = 16$ with the predictions of the effective-medium approximation (straight line).

Figure 3 presents the computed shear modulus μ versus p, the fraction of intact bonds, for ten realizations of the lattice of size $L = 16$, the largest lattice simulated in our previous study [17]. μ was normalized by its value at $p = 1$. There is no indication of a discontinuous phase transition as p_{ce} is approached, hence confirming the previous results.

Figure 4 presents a plot of $\ln \mu$ versus $\ln L$ for $L \leqslant 20$ at $p = p_{ce}$. We fitted the numerical results to

$$\mu \sim L^{-\delta}[1 + a_1/\ln(L) + a_2/L], \tag{6}$$

where $\delta = f/\nu_e$, and a_1 and a_2 are two constants. The terms in [ ] represent correction to scaling that is particularly important when L is relatively small [34]. We obtained the estimate $\delta = f/\nu_e \simeq 1.97$ (with $a_1 \simeq -0.12$ and $a_2 \simeq 0.03$) with a goodness of fit, $R^2 \approx 0.99$. These results are in complete agreement with our earlier results [17], although in the present work we used a much larger number of realizations, and added the results for lattices of size $L = 20$ that had not been simulated in our earlier study.

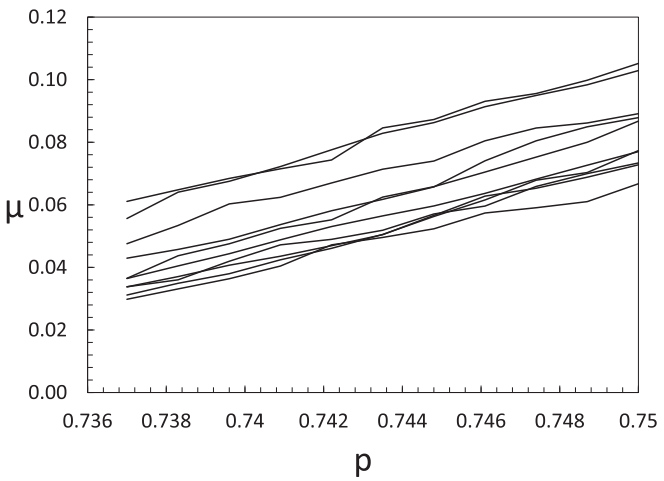

FIG. 3. Shear modulus μ of ten realizations of BCC lattice with linear size $L = 16$.

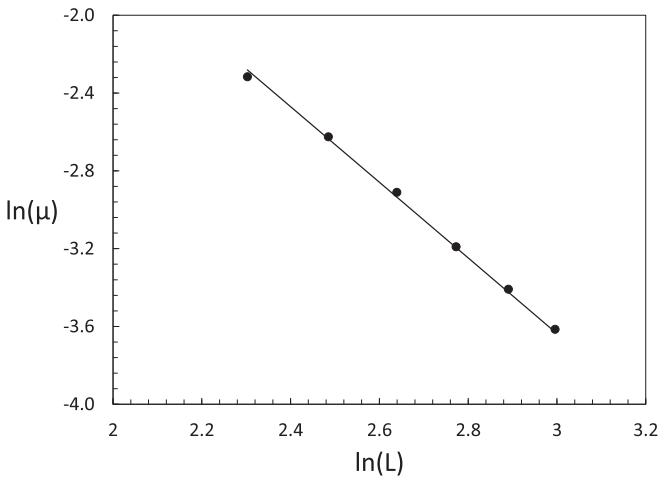

FIG. 4. Scaling of the shear modulus μ with the linear size L of the bcc lattice, with $L \leqslant 20$.

To further check the estimate of δ obtained by fitting the data to Eq. (6), we also fitted them to two simpler equations:

$$\mu \sim L^{-\delta}(a + bL^{-\alpha}), \tag{7}$$

$$\mu \sim L^{-\delta}[a + b(\ln L)^{-\alpha}], \tag{8}$$

where α is a correction-to-scaling exponent. Let us define $\chi^2 = \sum[(\text{data} - \text{model})/\text{data}]^2$, where "model" refers to the predictions of Eqs. (6)–(8) fitted to the numerical data. The fit of the data to Eq. (6) was obtained with $\chi^2 \approx 6 \times 10^{-5}$; Eq. (7) yielded $\delta \simeq 1.97$, $\alpha \simeq 1.36$, and $\chi^2 \simeq 4.4 \times 10^{-4}$, whereas we obtained $\delta \simeq 1.97$, $\alpha \simeq 1.62$, and $\chi^2 \simeq 4.9 \times 10^{-4}$. Thus, the three equations yield identical estimates for δ, but with a smaller χ^2 for Eq. (6). Interestingly, we obtained $a \simeq 1$ for both Eqs. (7) and (8), consistent with Eq. (6).

The "trouble" begins to emerge when much larger lattices are simulated. We show in Fig. 5 the results for two sets of realizations. For $0.75 \leqslant p \leqslant 1$ the shear modulus of all the realization decreases smoothly with p and, therefore, need not be shown, while for $p < 0.75$ we computed the elastic modulus in steps of size $\Delta p = 1.3 \times 10^{-3}$. Figure 5(a) compares the computed μ for ten realizations of the lattice of size $L = 70$, the largest one simulated in the present work. The ten realizations are nonpercolating at $p = 0.737$, indicated in the figure by not crossing the horizontal axis. Figure 5(b) presents the results for an ensemble of percolating realizations over exactly the same range of p. They have an essentially zero modulus with $\mu < 10^{-6}$ and show up as touching the horizontal axis. As both figures indicate, when *and only when* the size of the lattice is large enough do the discontinuous steps in the functional form of $\mu(p)$ emerge. Note that the flat part of the steps implies that it costs no energy to deform the lattice for the lower values of p until the next step is reached, which is due to free rotation of the bonds in the lattice. Note also that the length and position of the steps vary significantly among realizations, implying that averaging the results over the realizations is very difficult, and unreliable, regardless of the method used. We return to Fig. 5 shortly.

Note that the stairs in Fig. 5 should be completely horizontal, i.e., over the length of the stairs the change in the

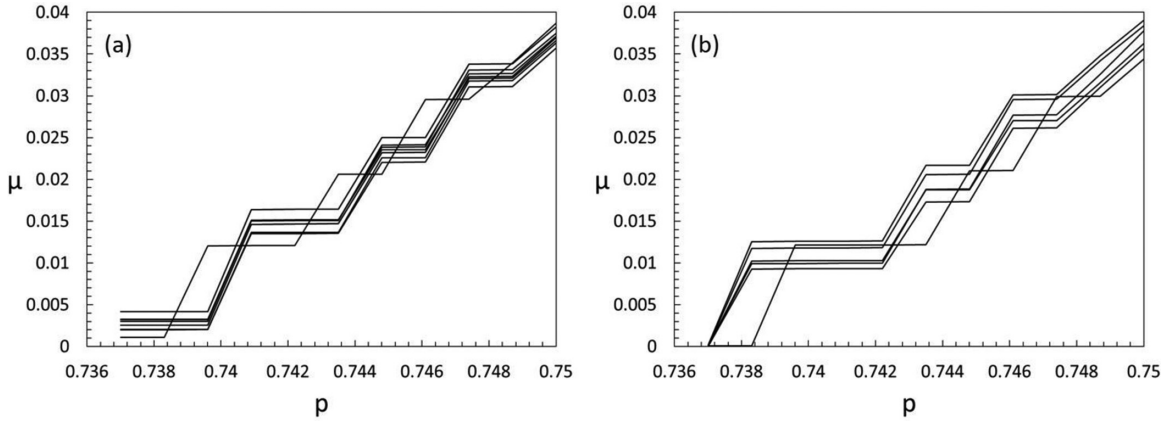

FIG. 5. Shear modulus of ten realizations of the bcc lattice of size $L = 70$ in the interval $p_{ce} = 0.737 \leqslant p \leqslant 0.75$. (a) Nonpercolating and (b) percolating realizations.

backbone should occur at no cost to the elastic energy of the system and, therefore, no change in the shear modulus, due to the (energetically) free rotations of the clusters of bonds. Numerically, however, the stairs do have a very small slope due to the convergence criterion used in the simulations. In the numerical simulations the solution of the governing equations for the nodal displacements at a given p is used as the initial guess for determining the solution at $p - \Delta p$. Given the very small value of Δp, over the length of a stair the nodal displacements change extremely slightly from p to $p - \Delta p$, less than 10^{-5}, well within the numerical tolerance. The overall effect is that the shear modulus is lower at $p - \Delta p$ over a given stair by a negligible amount. For example, in one realization of the $L = 70$ lattice, $\mu = 2.1935 \times 10^{-4}$ at $p = 0.741$, whereas $\mu = 2.1919 \times 10^{-4}$ at $p = 0.7397$.

To understand these results better and to provide numerical evidence in support of the above argument, we note that the total number of bonds, N_0, in the intact lattice (at $p = 1$) is $N_0 = Z(L-1)^3$ with $Z = 8$ being the coordination number. Thus, for the results shown in Fig. 3 with $L = 16$ we have $N_0 = 27\,000$ bonds, and the number of bonds removed at each step is $n_p = N_0 \Delta p = 27000 \Delta p$. With $\Delta p = 1.3 \times 10^{-3}$ for $p < 0.75$, each step of decreasing p by Δp removes about 35 bonds from the lattice. When 35 bonds are removed from the lattice, the decrease in the number of bonds in the backbone is larger than 35, because more bonds gain *free rotation* (at no cost to the elastic energy). Thus, by removing more bonds the nonlocal effect of the spatial distribution of the CFs is propagated, and a sample-spanning cluster with a larger number of freely rotating bonds emerges.

Figure 6(a) presents the variation of M_0, the number of bonds in the backbone, with p for $p < 0.75$ and $L = 16$, in one realization of the lattice. As expected, M_0 decreases more or less smoothly with decreasing p. Figure 6(b) shows the change $\Delta M_0 = M_0(p) - M_0(p - \Delta p)$ in number of bonds in the backbone at each step change of $\Delta p = 0.0013$, indicating that removing 35 bonds from the lattice at each step affects up to 204 bonds in the backbone in the same realization. Next, consider Figure 6(c), in which we plot the normalized variable $\Delta M_0/(N_0 \Delta p)$ versus p. Close to $p = 1$ the change in M_0 is about the same as the number of removed bonds at each step. Thus, removal of the bonds at high values of p has only a *local* effect. As lower values of p are approached, however, the ratio exceeds 1, implying that the effect of removal of the bonds on the backbone becomes far reaching and nonlocal. Moreover, for $p < 0.75$ the ratio has a strong nonmonotonic behavior, signaling that the backbone is very sensitive to bonds' removal.

To better demonstrate the significance of large lattice sizes to the emergence of the stepwise decrease of shear modulus with decreasing p, we compare in Fig. 7 the shear modulus $\mu(p)$ for three lattice sizes. These results are for a single realization of the lattice for each L. For $L = 30$ only one step emerges very close to p_{ce}. When the size is increased to $L = 50$, two steps are developed, whereas for $L = 70$ multiple steps emerge over the entire range of p that we consider. Thus, we may expect that if we extrapolate the behavior of the lattice of size $L = 70$ to larger ones, we will have continuous increase in the frequency and length of the steps, which would provide strong evidence that the steps connect for $p < 0.75$ and emerge as a large one, signaling a possible first-order transition. We will come back to this point shortly.

Further evidence for the possible first-order transition is presented in Fig. 8. Figure 8(a), which shows the average of μ for all the lattice sizes that were simulated at p_{ce}, with the average taken over the number of realizations generated for each L, indicates clearly that the slope changes for $L > 60$. Note that there is an upward jump in the data from $L = 56$ to $L = 60$ (the first solid circle in the figure). To further validate the data for $L = 60$, a separate set of simulations with 50 realizations was carried out. The average modulus μ for the first set at p_{ce} was 0.00544, whereas it was 0.00537 for the second set. The close agreement confirms the accuracy of the results for $L = 60$. The change in the slope is further verified by the data from larger sizes.

Another way of looking at the issue is provided in Fig. 8(b), where we compare $\mu(p)$ versus $p - p_{ce}$ for two sizes L near p_{ce}. One is for $L = 16$, indicating smooth power-law vanishing of $\mu(p)$, consistent with Fig. 4. The second one presents the averaged $\mu(p)$ for $L = 70$. Since in this case $\mu(p)$ decreases in a stepwise manner, we used the middle of the steps for each $p - p_{ce}$ and performed the averaging. In contrast with the results for $L = 16$, there is a large jump in the value of $\mu(p)$ right before it vanishes at $p = p_{ce}$, hence

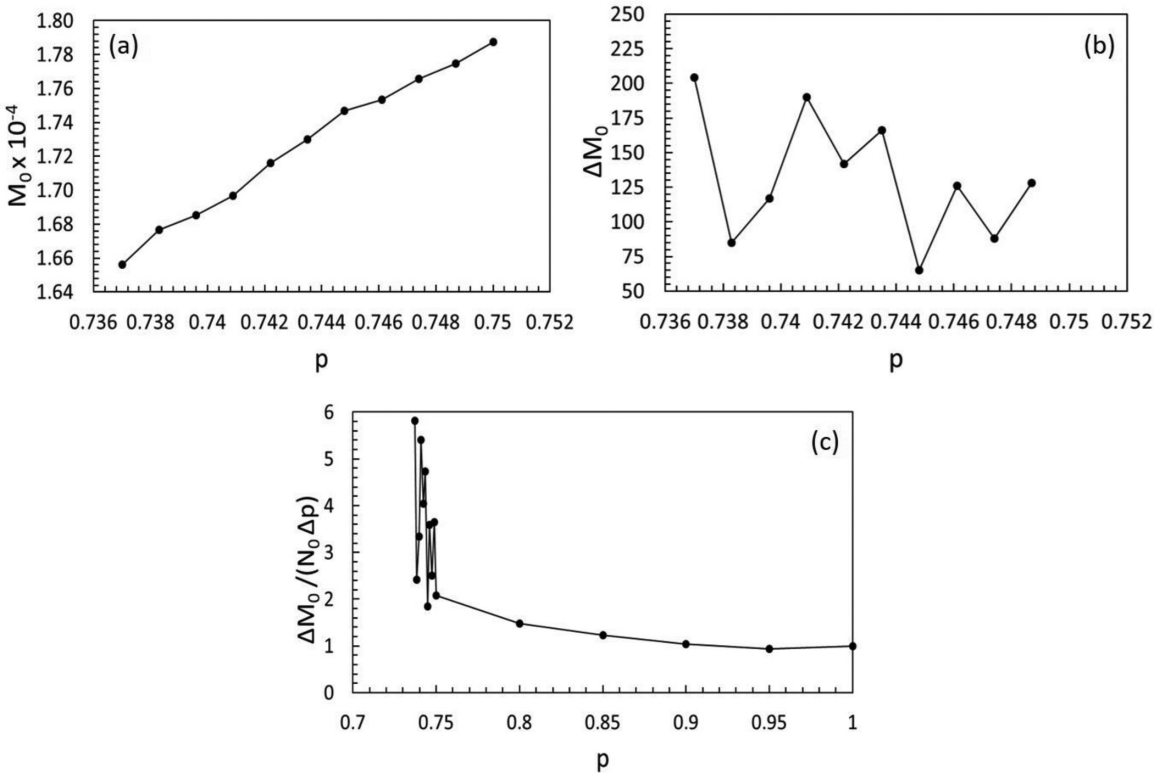

FIG. 6. (a) Dependence of the number of bonds, M_0, in the backbone on the fraction p of the bonds. (b) The change in the number of bonds, $\Delta M_0 = M_0(p) - M_0(p - \Delta p)$, in the backbone versus p. (c) Normalized change in the number of the backbone bonds, $\Delta M_0/(N_0 \Delta p)$ versus p, where Δp is the change in p between two successive steps, and N_0 is the number of bonds at $p = 1$. All the results are for a lattice of linear size $L = 16$.

providing another indication for the possibility of a first-order phase transition.

A third way of studying the order of the phase transition at p_{ce} is by studying the decrease in the modulus μ with smaller Δp intervals of 0.0002, instead of the 0.0013 used so far, which demonstrates clearly that as the size L increases, the steps in μ combine and a larger final jump to no rigidity is formed at p_{ce}. This is shown in Fig. 9 where we compare the results for one typical realization with $L = 30$ and $L = 70$ very close to the threshold. We note that the small steps for $L = 30$, which are detectable only at the higher resolution (smaller Δp), combine and form a large horizontal step for $L = 70$. The final step at $p = 0.736$ for $L = 70$ has grown in size relative to that for $L = 30$. Thus, Fig. 9 provides further evidence for the proposed phase-transition picture, namely, that as L increases, the bcc lattice with only CFs undergoes a first-order transition.

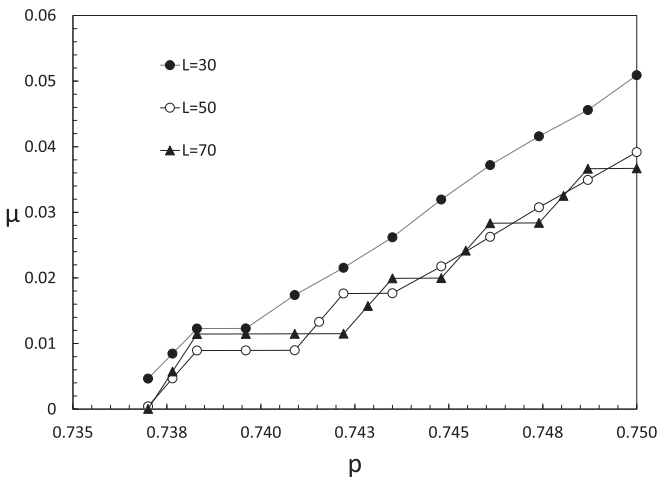

FIG. 7. Emergence of discontinuous steps in the dependence of the shear modulus μ on p as the size L of the lattice increases.

C. The backbone

As already pointed out, the moment M_0 of the force distribution represents the total number of bonds in the backbone, the stress-transmitting part of the sample-spanning rigid cluster. Therefore, for $q = 0$ the exponent $\tilde{\tau}_q$ is equal to the fractal dimension D_{bb} of the backbone. To obtain a precise estimate of D_{bb}, and taking into account the finite-size effects, we write

$$M_0 \propto L^{-D_{bb}}[1 + a_1/\ln(L) + a_2/L]. \tag{9}$$

Figure 10 presents the results. Admittedly, the range of L is small, with only a factor of about 2.5 variations. It is, however, not currently possible, for us at least, to simulate any lattice with a linear size $L > 70$. The fit of M_0 to Eq. (9) yielded $D_{bb} \simeq 3.02 \pm 0.08$, implying that the backbone is completely compact. A compact backbone implies a first-order phase transition for the elastic moduli at p_{ce}. Thus, this provides further evidence that the transition in the elastic moduli at p_{ce} may be first order.

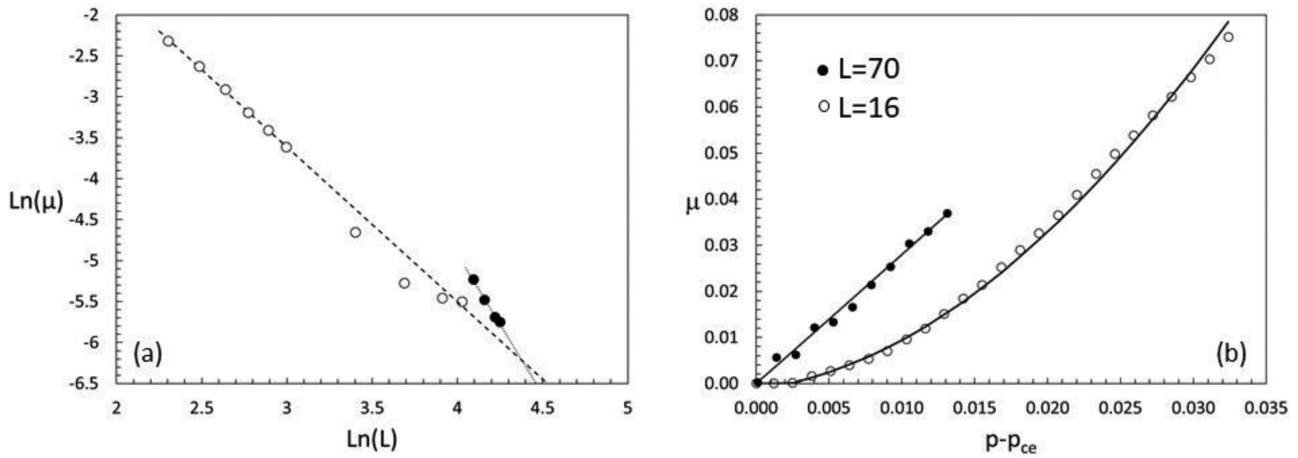

FIG. 8. (a) Dependence of the average shear modulus μ on the size L of the bcc lattice at the rigidity threshold p_{ce}. Observe the change of slope for $L \geqslant 60$, as well as the behavior of μ for the largest L. (b) Comparison of the dependence of the averaged shear modulus $\mu(p)$ on $p - p_{ce}$ for a lattice of linear size $L = 16$ (open circles) and $L = 70$ (solid circles). Observe the large jump in $\mu(p)$ for $L = 70$ at the last point before $p - p_{ce} = 0$ and compare it with that for $L = 16$.

D. Bimodality and first-order phase transition

In studies of liquid-gas phase transitions it was suggested [35,36] that bimodality of the distribution of the order parameter near a critical point is a signature of a first-order phase transition in finite systems, although counterarguments [37] and counterexamples [38] have also been suggested. Bimodality in the context of the present problem means that if the transition at p_{ce} is first order, then there is a region in the vicinity of p_{ce} in which both percolating and nonpercolating lattices are possible. In other words, if we generate an ensemble of realizations at, for example, $p = 0.739$, percolation has already occurred in a fraction of the realizations, whereas in the remaining fraction percolation has not occurred.

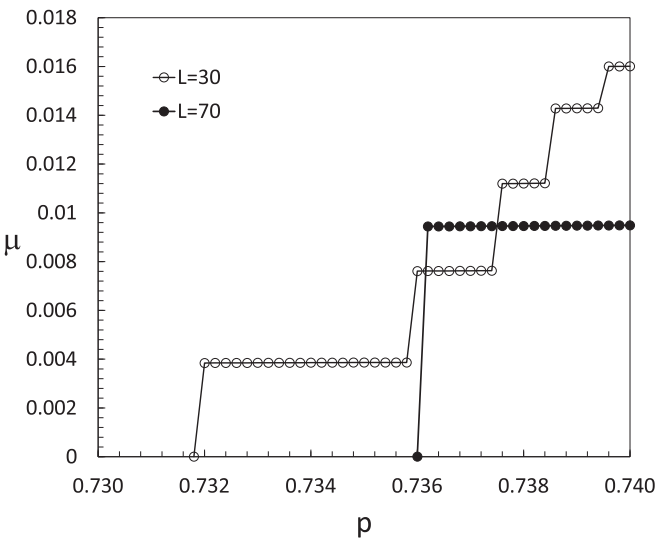

FIG. 9. Comparison of the stepwise decrease in the shear modulus μ very near the rigidity threshold p_{ce} for two lattice sizes L. Note the single step in the lattice of size $L = 70$, after which μ sharply drops to zero, and compare it with the multiple steps for $L = 30$.

This is indeed what the simulations indicate. We already pointed out that the two sets of results shown in Fig. 5 represent ensembles of percolating and nonpercolating lattices over the same interval of p. At $p = p_{ce}$ about 20% of the realizations are percolating, while the rest are not.

E. Scaling of the average step size

The last evidence for the possible first-order phase transition of the elastic moduli at p_{ce} is provided by the scaling of the mean step size S with the linear size L of the lattice at p_{ce}. Figure 11 presents the results, which indicate that the mean step size increases with L at the rigidity percolation threshold. Thus, as L becomes very large, so also does the step size, implying that an eventual large jump in the elastic moduli from a nonzero value to zero emerges, hence supporting a first-order phase transition.

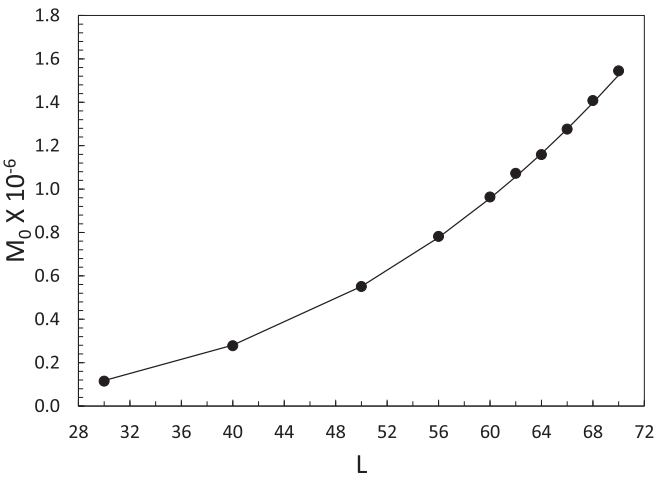

FIG. 10. Scaling of the mass M_0 with the linear size L of the bcc lattice at its rigidity threshold p_{ce}.

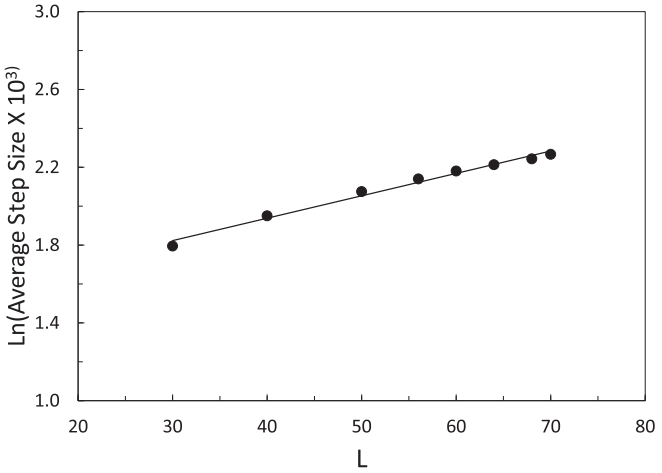

FIG. 11. Scaling of the average step size with the linear size of the bcc lattice at its rigidity threshold p_{ce}.

The results presented in Fig. 11 may be used to obtain a rough estimate of the minimum size L to observe a clear step in the value of the shear modulus of the lattice. The straight line in the semilogarithmic plot of Fig. 11 is described by $L \simeq 86.7 \ln(S) + 471$. The size (height) of the step is the value of the shear modulus for a particular value of p. Thus, for example, for $p = 0.7485$ (the numerical estimate of p_{ce} suggested by Chubynsky and Thorpe [32]), $\mu \approx 0.033$, which means $L \approx 175$, about 2.5 times larger than the largest lattice size that we can currently simulate. For $p = 0.737$ (our estimate of p_{ce}), $\mu \approx 0.012$ and, therefore, $L \approx 90$.

V. SUMMARY

Rigidity percolation with central forces is a nonlocal phenomenon. As the rigidity percolation threshold is approached, long-range, nondecaying correlations are built up. Such correlations give rise to compact, nonfractal structures. The absence of fractal, scale-invariant clusters, the hallmark of second-order phase transitions, implies that both the topological properties of rigidity percolation and its elastic moduli should undergo a first-order phase transition at p_{ce}. The results presented in this paper support this for at least bcc lattices, but we emphasize that one should study still larger lattices. In addition, whether this is true for other regular 3D lattices remains to be studied.

In small systems, however, the boundary effects interfere with the nonlocal nature of the rigidity percolation. As a result, only when such effects diminish in large lattices does the true nature of the phase transition emerge. This explains the earlier results [17] with relatively small bcc lattices that had indicated a second-order phase transition for the elastic moduli at p_{ce}. The results presented in this paper support this picture, although simulations with larger lattices would still be desirable. The results are also in agreement with the previous theoretical analysis [21] and numerical simulation [24,25].

ACKNOWLEDGMENTS

S.A. gratefully acknowledges the University of Texas STARs grant for financial support. We thank the two anonymous referees for many useful suggestions that helped us improve the results and clarify a few aspects of the problem studied.

[1] M. F. Thorpe, Continuous deformation in random networks, J. Non-Cryst. Solids **57**, 355 (1983).
[2] S. Feng and P. N. Sen, Percolation on Elastic Networks: New Exponent and Threshold, Phys. Rev. Lett. **52**, 216 (1984).
[3] Y. Kantor and I. Webman, Elastic Properties of Random Percolating Systems, Phys. Rev. Lett. **52**, 1891 (1984).
[4] S. Feng, P. N. Sen, B. I. Halperin and C. J. Lobb, Percolation on two-dimensional elastic networks with rotationally invariant bond-bending forces, Phys. Rev. B **30**, 5386 (1984).
[5] S. Feng and M. Sahimi, Position-space renormalization for elastic percolation networks with bond-bending forces, Phys. Rev. B **31**, 1671 (1985).
[6] S. Arbabi and M. Sahimi, Elastic properties of three-dimensional percolation networks with stretching and bond-bending forces, Phys. Rev. B **38**, 7173 (1988).
[7] G. R. Jerauld, Flow and transport in chaotic media: Four case studies, Ph.D. thesis, University of Minnesota, Minneapolis, 1985.
[8] S. Feng, M. F. Thorpe, and E. Garboczi, Effective-medium theory of percolation on central-force elastic networks, Phys. Rev. B **31**, 276 (1985).
[9] E. J. Garboczi and M. F. Thorpe, Effective-medium theory of percolation on central force elastic networks. II. Further results, Phys. Rev. B **31**, 7276 (1985).
[10] E. J. Garboczi and M. F. Thorpe, Effective-medium theory of percolation on central-force elastic networks. III. The superelastic problem, Phys. Rev. B **33**, 3289 (1985).
[11] E. J. Garboczi and M. F. Thorpe, Density of states for random central-force elastic networks, Phys. Rev. B **32**, 4513 (1986).
[12] M. F. Thorpe and E. J. Garboczi, Site percolation on central-force elastic networks, Phys. Rev. B **35**, 8579 (1987).
[13] O. Pla, R. Garcia-Molina, F. Guinea, and E. Louis, Properties of elastic percolating networks in isotropic media with arbitrary elastic constants, Phys. Rev. B **41**, 11449 (1990).
[14] S. Arbabi and M. Sahimi, Absence of universality in percolation models of disordered elastic media with central forces, J. Phys. A **21**, L863 (1988).
[15] A. Hansen and S. Roux, Universality class of central-force percolation, Phys. Rev. B **40**, 749 (1989).
[16] M. A. Knackstedt and M. Sahimi, On the universality of geometrical and transport exponents of rigidity percolation, J. Stat. Phys. **69**, 887 (1992).
[17] S. Arbabi and M. Sahimi, Mechanics of disordered solids. I. Percolation on elastic networks with central forces, Phys. Rev. B **47**, 695 (1993).
[18] D. J. Jacobs and M. F. Thorpe, Generic Rigidity Percolation: The Pebble Game, Phys. Rev. Lett. **75**, 4051 (1995).

[19] C. Moukarzel and P. M. Duxbury, Stressed Backbone and Elasticity of Random Central-Force Systems, Phys. Rev. Lett. **75**, 4055 (1995).

[20] C. Moukarzel and P. M. Duxbury, Comparison of rigidity and connectivity percolation in two dimensions, Phys. Rev. E **59**, 2614 (1999).

[21] S. P. Obukhov, First Order Rigidity Transition in Random Rod Networks, Phys. Rev. Lett. **74**, 4472 (1995).

[22] M. Sahimi and S. Mukhopadhyay, Scaling properties of a percolation model with long-range correlations, Phys. Rev. E **54**, 3870 (1996).

[23] M. A. Knackstedt, M. Sahimi, and A. P. Sheppard, Invasion percolation with long-range correlations: First-order phase transitions and nonuniversal scaling properties, Phys. Rev. E **61**, 4920 (2000).

[24] C. Moukarzel, P. M. Duxbury, and P. L. Leath, Infinite-Cluster Geometry in Central-Force Networks, Phys. Rev. Lett. **78**, 1480 (1997).

[25] C. Moukarzel, P. M. Duxbury, and P. L. Leath, First-order rigidity on Cayley trees, Phys. Rev. E **55**, 5800 (1997).

[26] J. Chalupa, P. L. Leath, and G. R. Reich, Bootstrap percolation on a Bethe lattice, J. Phys. C **12**, L31 (1979).

[27] P. M. Kogut and P. L. Leath, Bootstrap percolation transitions on real lattices, J. Phys. C **14**, 3187 (1981).

[28] M. Sahimi and T. S. Ray, Transport through bootstrap percolation clusters, J. Phys. I France **1**, 685 (1991).

[29] D. J. Jacobs and M. F. Thorpe, Generic rigidity percolation in two dimensions, Phys. Rev. E **53**, 3682 (1996).

[30] P. M. Duxbury, D. J. Jacobs, M. F. Thorpe, and C. Moukarzel, Floppy modes and the free energy: Rigidity and connectivity percolation on Bethe lattices, Phys. Rev. E **59**, 2084 (1999).

[31] M. V. Chubynsky and M. F. Thorpe, in *Physics and Applications of Disordered Materials*, edited by M. Popescu (INOE, Bucharest, Romania, 2002), p. 229.

[32] M. V. Chubynsky and M. F. Thorpe, Algorithms for three-dimensional rigidity analysis and a first-order percolation transition, Phys. Rev. E **76**, 041135 (2007).

[33] M. Sahimi and S. Arbabi, Force distribution, multiscaling and fluctuations in disordered elastic media, Phys. Rev. B **40**, 4975 (1989).

[34] M. Sahimi and S. Arbabi, On correction to scaling for two- and three-dimensional scalar and vector percolation, J. Stat. Phys. **62**, 453 (1991).

[35] Ph. Chomaz, F. Gulminelli, and V. Duflot, Topology of event distributions as a generalized definition of phase transitions in finite systems, Phys. Rev. E **64**, 046114 (2001).

[36] Ph. Chomaz and F. Gulminelli, First-order phase transitions: Equivalence between bimodalities and the Yang-Lee theorem, Physica A **330**, 451 (2003).

[37] O. Lopez, D. Lacroix, and E. Vient, Bimodality as a Signal of a Liquid-Gas Phase Transition in Nuclei, Phys. Rev. Lett. **95**, 242701 (2005).

[38] K. A. Bugaev, A. I. Ivanytskyi, V. V. Sagun, and D. R. Oliinychenko, Is bimodality a sufficient condition for a first-order phase transition existence, Phys. Part. Nucl. Lett. **10**, 508 (2013).